HEAT SENSOR

HARSH ENVIRONMENT ADAPTABLE THERMIONIC **SENSOR**

Final Report

Reporting Period Start Date: 10/01/13
Reporting Period End Date: 5/31/16

Submitted by

Scott J. Limb
Palo Alto Research Center
3333 Coyote Hill Road
Palo Alto, CA 94304

This work was sponsored by

National Energy Tech Lab (NETL) / Department of Energy
DE-FE0013062
Program Manager: Barbara Carney, NETL, Morgantown, WV

DISCLAIMER

ABSTRACT

This document is the final report for the "***H*ARSH *E*NVIRONMENT *A*DAPTABLE *T*HERMIONIC SENSOR"** project under NETL's Crosscutting contract DE-FE0013062. This report addresses sensors that can be made with thermionic thin films along with the required high temperature hermetic packaging process. These sensors can be placed in harsh high temperature environments and potentially be wireless and self-powered.

TABLE OF CONTENTS

LIST OF FIGURES

LIST OF TABLES

EXECUTIVE SUMMARY

Market Need: As identified in the FOA, sensing process parameters such as temperature, pressure, flow rate, heat flux, and strain/stress at very high temperature (750-1600 ^{0}C) and pressure (1000 psi) open to harsh fuel, oxidizer and combustion product environments is very difficult or not possible with the technologies available today. It is an important problem in high performance combustion systems, such as aircraft turbines, natural gas engines, compressors and large propellers. In most of these cases, wires running to these sensors for supplying power and reading sensor electrical response are a great inconvenience and compromise to the safety and integrity of the system. It is therefore desirable to have a sensor platform that works in such an environment that harvests its own energy, has its own high temperature electronics and sends out signals wirelessly.

General Technical Approach: Certain alloys that have melting point higher than 1600 °C develop a space charge in vacuum without the need for heating as required in traditional thermionic tubes. Such alloys and metals can be used as thermionic emitters and receivers at such temperatures without the need for an external heating element. Structures made out of such metals and alloys can be encapsulated in high temperature high vacuum ceramics. Encapsulation and interconnection with such ceramics are routinely done at the lower end of the temperature range of interest (750 °C) and with appropriate material choices, the temperature ceiling can be extended to the higher end of the range (1600 °C). Such structures will normally be evacuated before sealing to facilitate thermionic emission and electron optics. By applying an appropriate potential across the emitter and receiver a thermionic electron current can be established. Everything else remaining constant, the thermionic current increases with temperature, and such a structure can therefore be used as a temperature sensor. Thermionic pressure sensors can also be made using membrane deflection approaches. The thermionic current will vary depending on the degree of deflection thus measuring pressure. A combination of temperature and pressure sensors can be configured to produce other desired sensors, such as flow rate and heat flux.

Key Technology Development: Since thermionics is a well understood technology used for over a century in applications such as vacuum tube electronics, the critical development will be forming an high temperature hermetic package that will not only protect the thermionic material from fouling during use but more importantly during the packaging process. PARC has focused much of the research into developing a reliable high temperature packaging process for thermionic thin films. This key technology can be applied to other sensors that need to be protected in harsh high temperature environments.

Project Goals and Accomplishment:

1. ***Develop an high temperature hermetically sealed packaging process:*** PARC has developed an high temperature hermetic package method that can be thermally cycled and held at 1300 °C for over 3000 hrs with a leak rate less than 1 e-7 bar cc/s. Using alumina as the package material, a propriety hermetic sealing paste and high temperature packaging method was developed to ensure a proper vacuum and protection from the harsh reactor environment.

2. ***Develop and demonstrate the operation of the thermionic element:*** This is the basic building block of the HEAT technology platform, requiring architecture design, materials selection, and fabrication process development. PARC has developed thin film thermionic devices that can be used to measure temperature, pressure, and harvest energy.
3. ***Develop and validate the performance of a functional packaged temperature and pressure sensor:*** The HEAT sensor will integrate thermionic elements into a functional hermetic package capable of measuring temperature and pressure over the target range of environmental conditions. Processes have been developed to ensure a clean thermionic surface during packaging. Thermionic measurements were achieved with this packaging process and further development is needed to improve the overall reliability of the thermionic material.
4. ***Develop and demonstrate the pathway to multi-parameter wireless self-powered sensor:*** The HEAT sensor will incorporate energy harvesting, wireless data transmission, and internal vacuum capabilities for a completely wireless configuration with a stretch goal to advance as far as possible towards demonstration of a fully integrated sensor package. Initial concept designs and experimental validation of the key enablers for these additional capabilities were completed.

TECHNICAL PRESENTATION

Ultra-High Temperature Hermetic Package

Test Procedure and Apparatus. Hermeticity testing requires very sensitive pressure sensors and vacuum systems. An MTI 1700 °C vacuum oven with a Pfeiffer turbo pump (Figure 2) was used to measure the hermeticity of the package and sealant.

Figure 2. Pfeiffer Turbo Pump and Two MTI 1700 °C Vacuum Oven

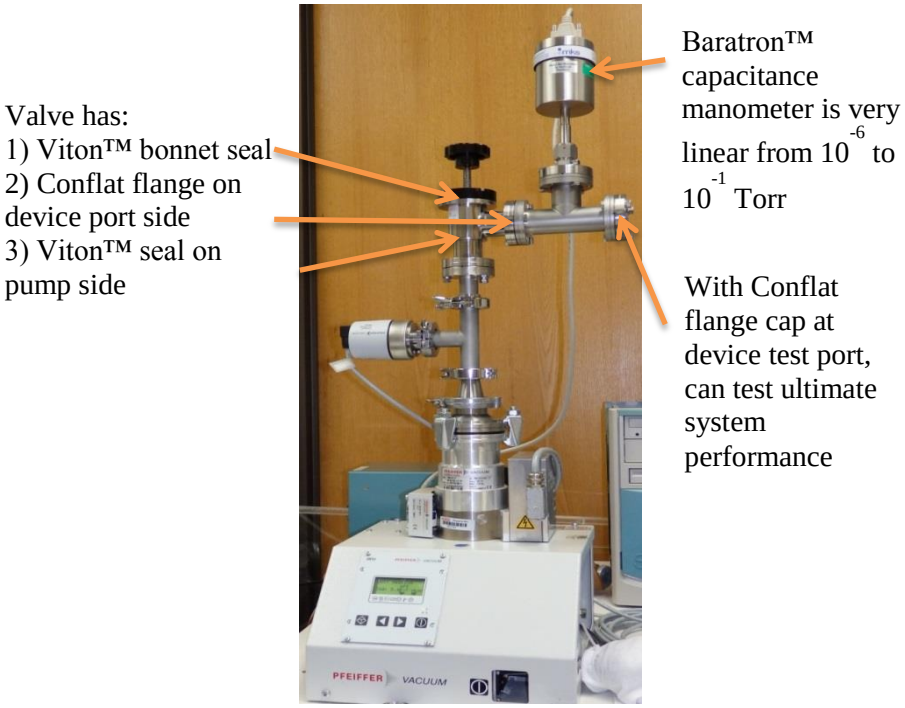

Figure 1. Baseline Measurement Setup and Configuration

Baseline Pressure Rise Measurement. Extensive reconfiguration of the pumping system had to be made in order to reduce the rate of rise to acceptable levels. The Viton o-rings were causing outgassing issues and thus we had to change many of the seals. Additionally a new pressure gauge was installed for this test. The final setup and changes can be seen in Figure 1.

In Figure 3, the graph shows the base pressure and pressure rise for our vacuum test system. The system was pumped to an adequately low pressure and isolated from the pump. Two different endcaps were used for comparison. The first cap was all metal with a metal o-ring seal. The second cap had a Viton o-ring with a closed end ceramic tube. The entire vacuum system was sealed using metal o-rings to avoid any Viton outgassing. Both baseline measurements are below the 1E-04 mbar*cc/s milestone and thus our measurement sensitivity is more than adequate for our test structures. The metal cap baseline was measured to be 2.4E-05 mbar*cc/s and the ceramic cap baseline was 3.2E-05 mbar*cc/s. As a reference, a sample that was sealed using a prototype ceramic paste was also tested. This sample as expected had an higher leak rate than the baseline. For all samples tested, if the pressure measured less than 1E-4 mbar after 5 mins then the leak up rate was adequate to continue.

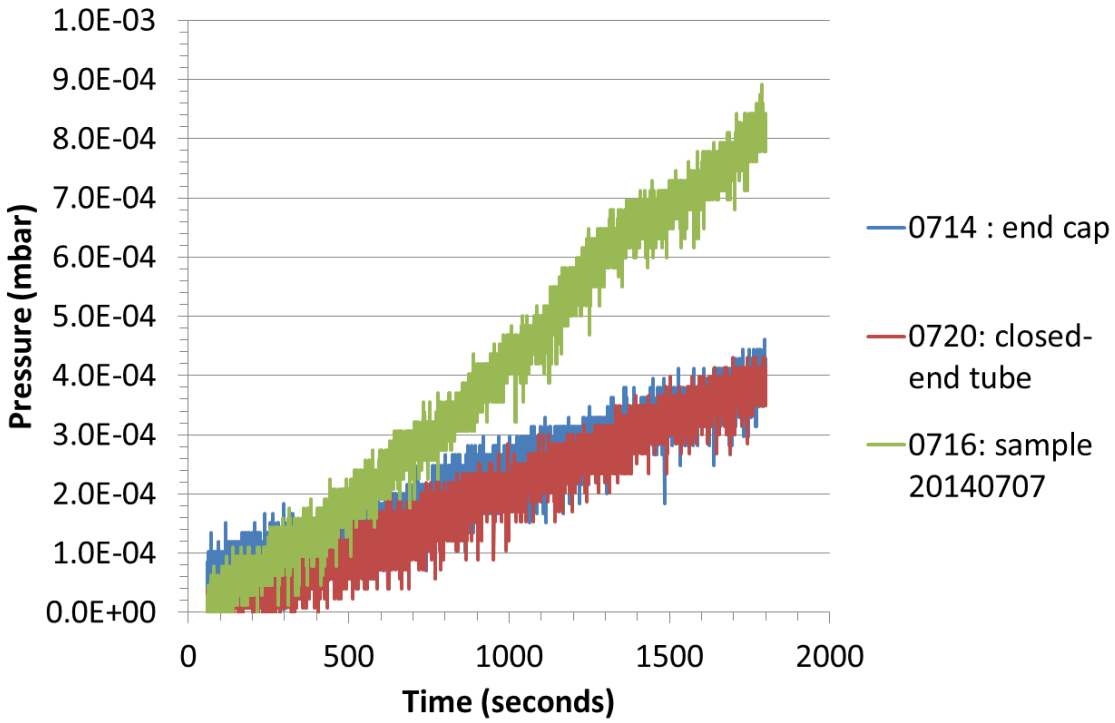

Figure 3. Pressure rise measurements for metal and ceramic caps. 0714 :end cap is a metal cap; 0720:closed-end tube is a ceramic cap; 0176:sample is sealed tube using a sealant.

Hermetic Sealant. Although metal layers are typically used for high vacuum hermetic sealing, our specific application requires the sealant to withstand high temperatures >1300 °C and harsh oxidizing environments. We have chosen to explore various ceramic pastes with high purity

alumina as the package material. The test method can be seen in Figure 4. The sealing paste is applied between a ceramic plate and tube. Both high purity aluminia items were procured from Coorstek. After application, the paste is air dried and furthered cured according to specification.

Figure 4. Sealant Paste Screening Test at Room Temperature

In Table 1, several materials that have been tested are shown. Base pressures at room temperature were measured for all the samples. If the seal integrity was adequate, we would expect the base pressure to be below 1E-4 mbar with the Pfieffer turbo pump connected. As expected stock alumina adhesives from Aremco and Cerabond did not form the proper seals. Although the cure temperature was low at 400C, the composition of the material created large pores after curing.

Table 1. Base Pressure Results for Various Hermetic Sealant Materials

Material	**Vendor**	**Cure Temp(°C)**	**Base Pressure Results at Room Temperature (mbar)**
Various Stock Items	Aremco	400	Non-sealing
Various Stock Items	Cerabond	400	Non-sealing
Special Order Alumina Paste -v1 and v2	Electro Science Lab	1500	3.4E-4 to 1.0 E-3
Special Order Barium Aluminosilicate	Aremco	1350	< 1E-4
PARC Paste	PARC	1400	< 1E-4

In order to eliminate any pores from forming, a melting component was added. Two custom pastes from Electro Science Labs were tested. Both formulations used alumina particles as the support structure and silica as the binder. In order to melt the silica component, the formulation needed was cured at 1500 °C. Although the porosity was eliminated, structural defects in the sealing process were noticed. In Figure 5. Electro Science Paste after 1500C Cure, delamination and stress cracks can be seen after curing. Stress cracks can result from a CTE mismatch but delamination might have other sources. Indeed upon further investigation, the initial drying process which removes the solvent caused the seal area to shrink and delaminate. In Figure 6, tests were done using glass plates in order to visually inspect the adhesion between the paste and components. Initially the paste wetted the surfaces well but after drying a clear delaminated area can be visible. Thus any sealants will need to have good CTE matching properties and surface wetting behavior.

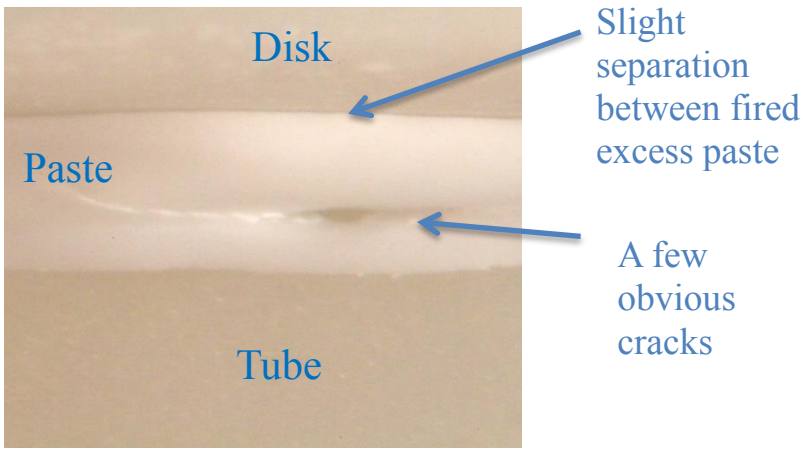

Figure 5. Electro Science Paste after 1500C Cure

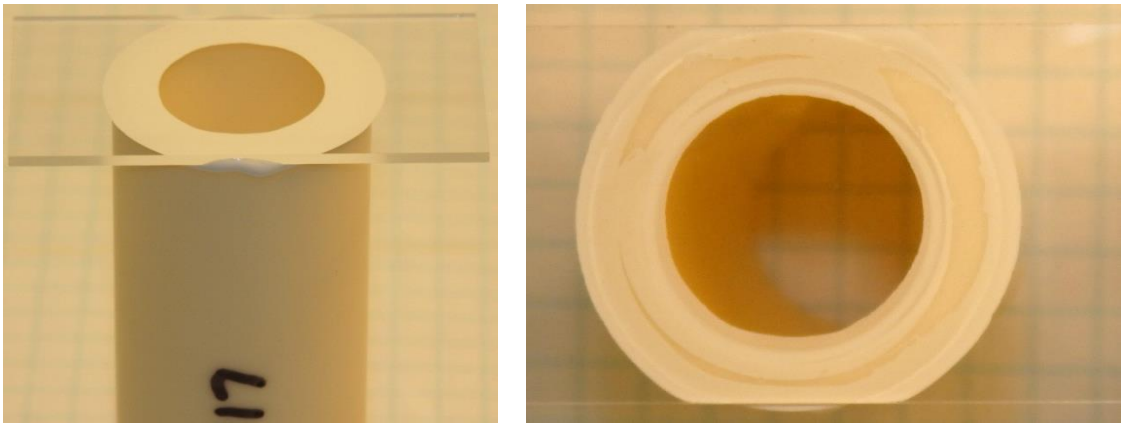

Sample after sealing
but before any drying

Sample after drying (<300 C bake)
Delamination is clearly visible

Figure 6. Delamination from Sample Drying

Aremco formulated a paste with barium aluminosilicate which had good CTE matching and wetting properties. For sealing integrity testing, the same sample was thermally cycled and tested for hermeticity at room temperature. The thermal cycles were As Cured, 1000 °C, 1100 °C, 1150 °C, 1200 °C, and 1250 °C. In Figure 7, the pressure rise versus time for various thermal cycling runs is charted. Although the thermal cycling was done in sequence from low to high, no systematic seal degradation was seen. In Table 2 the net leak up rate (mbar*cc/s) for

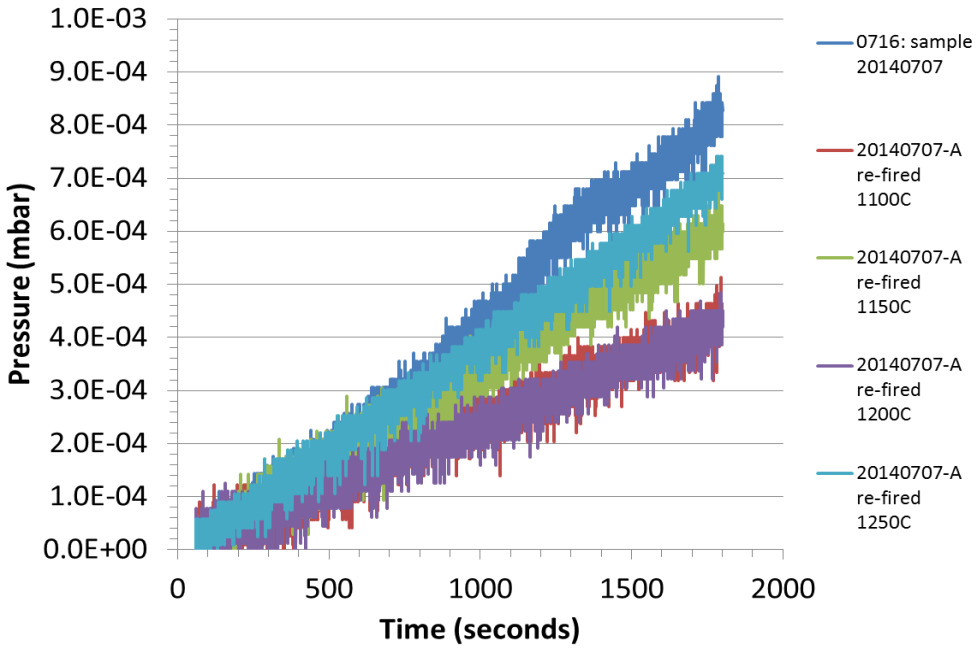

Figure 7. Barium aluminosilicate paste from Aremco. Pressure vs time measurement for various thermal cycling

each sample can be calculated by subtracting the background leak up rate. For all the samples, the net leak up rate was much less than 1E-04 mbar*cc/s which is defined as this project's target milestone. This value represents an hermeticity level that can be used for thermionic emissions. Furthermore, all six thermal cycles did not change the seal integrity. Since the measurements were done at room temperature, only thermal cycling behavior was measured. For practical operational limits, we do not expect continuous use to go beyond 1150 °C, since Barium Aluminosilicate melts at 1265 °C.

Table 2. Net Leak Up Rate for Aremco's Barium Aluminosilicate Sealant

Sample	**Description**	**Leak Up Measured (mbar*cc/s)**	**Net Leak Up (mbar*cc/s)**
Closed-end tube	Baseline	3.2 E-05	0
20140707-A	Aremco-Special Order – As Cured	6.9 E-05	3.7 E-05
20140715-A	Aremco-Special Order – As Cured	3.5 E-05	2.4 E-06
20140707-A	1100C thermal cycle	3.4 E-05	1.8 E-06
20140707-A	1150C thermal cycle	5.0 E-05	1.7 E-05
20140707-A	1200C thermal cycle	3.3 E-05	6.7 E-07
20140707-A	1250C thermal cycle	5.7 E-05	2.5 E-05

Although, the Aremco paste with Barium Aluminosilicate showed promise, an usable operating temperature of the sealant needs to be higher. In order to increase this operational window, PARC has developed a paste with continuous operation up to 1300 °C.

Pressure rise tests were done at temperature using the MTI furnace and a 24" length tube (Figure 9). For the experiment, a 24" alumina tube with an outer diameter of 1" was sealed to an alumina disk. The disk end was placed at the center of the MTI furnace tube and subjected to repeated thermal cycling and continuous operation at 1300 °C. During the entire operation, the ceramic tube's open end was connected to a pressure gauge and turbo pump (Figure 8). This pressure rise measurement setup is consistent with all room temperature measurements.

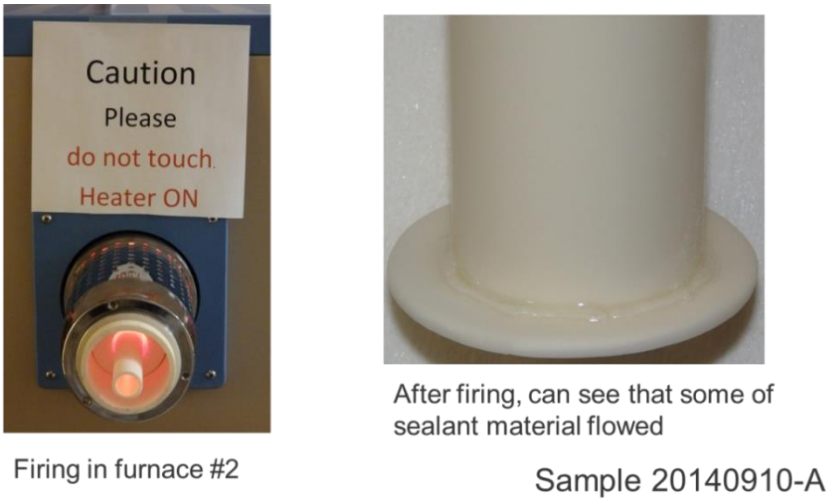

Figure 9. Sealed disk to tube experimental setup. Tube length was 24" with an OD of 1". The disk end was placed at the center of the furnace tube

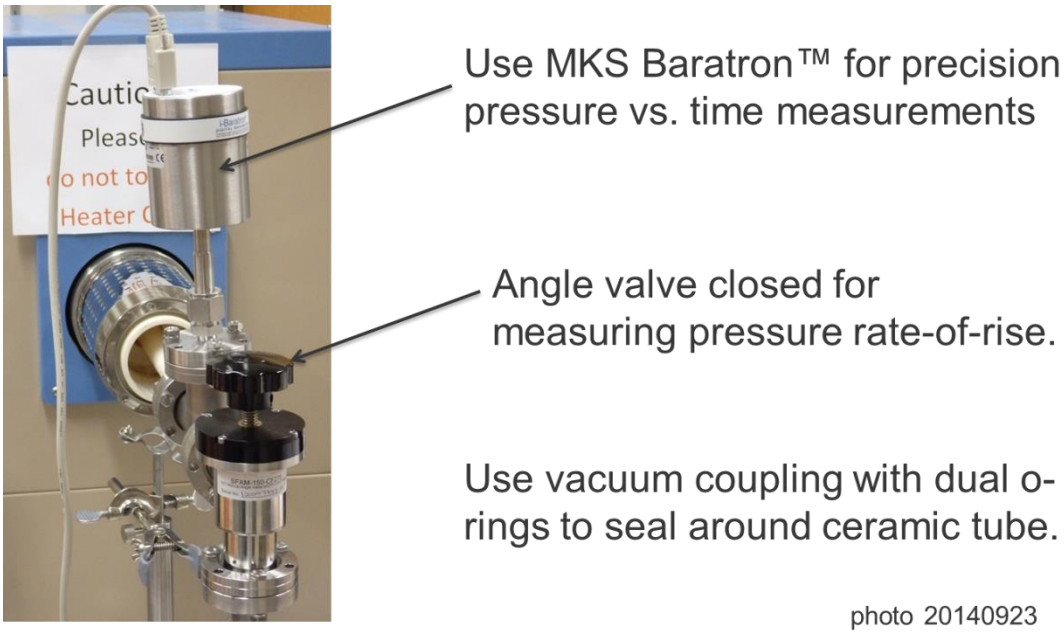

Figure 8. Pressure measurement and turbo pump setup.

The PARC hermetic paste sample soaked for over 2500 hrs at 1300 °C. During the 2500 hrs span (Figure 10), the sample was taken to room temperature once and repeatedly cycled between 1000 °C to 1300 °C. All data measurement after 500 hrs of soak were better than the milestone specification of 1e-7 bar*cc/s.

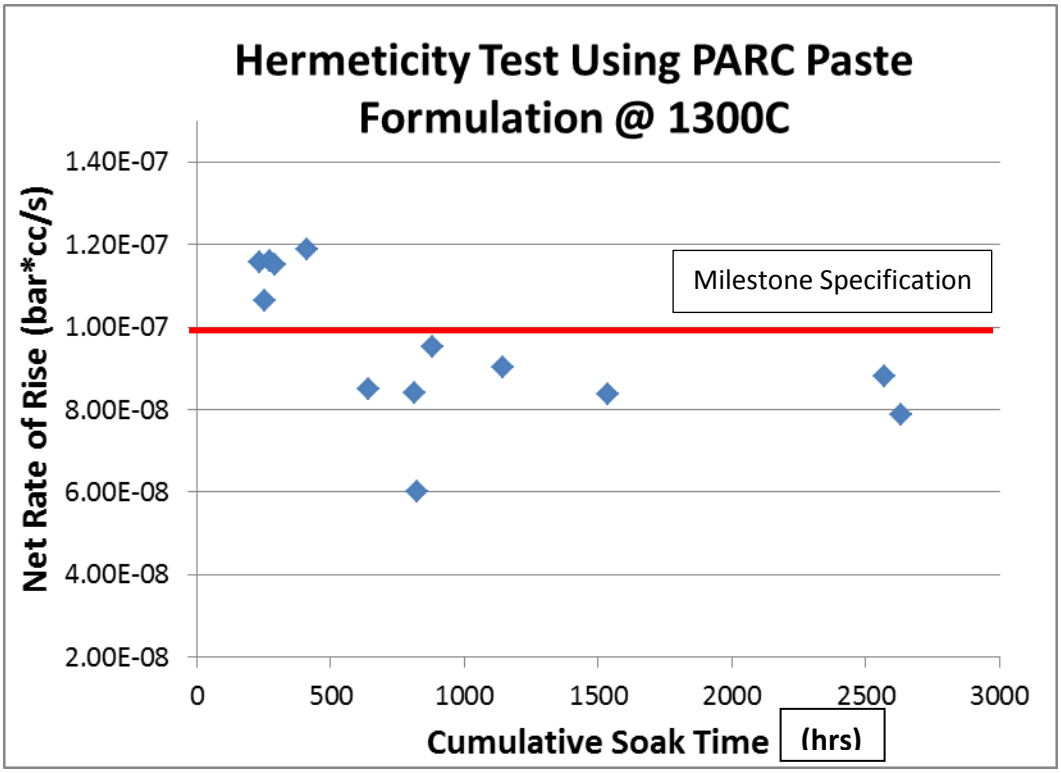

Figure 10. PARC Paste Hermeticity Test at Operational Temperature of 1300 °C. Each data point represents a thermal cycling run.

Thin Film Thermionic Development

Thermionic Concept. Thermionic emission is the heat induced flow of electrons from a metal surface. It occurs when the thermal energy of the electrons exceeds the binding force, i.e. work function, of the metal. Thermionic emission is the well understood process that is the basis for vaccuum tubes, where the released electrons are collected on a positively charged anode. In conventional applications, a heating coil is used to heat the metal surface to a sufficient temperature for thermionic emission to occur. For the HEAT sensor technology proposed here, we take advantage of the high temperatue environment to naturally induce thermionic emission from the cathode (Figure 11 (a)), and measure the resulting current on the anode (Figure 11 (b)) with the aid of a small bias voltage. The magnitude of the current is directly correlated to the temperature of the cathode, providing a simple but effective temperature sensor. The device can be designed such that the flow of electrons from the cathode to the anode is modulated by an external condition (e.g. pressure) to enable the measurement of a

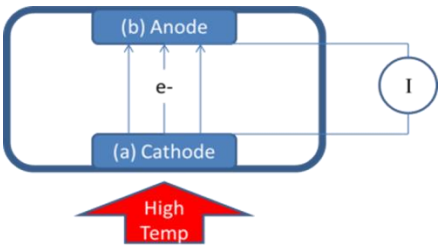

Figure 11. HEAT Thermionic Concept

wide range of process conditions. In the HEAT thermionic device, the thermionic emission is governed by Richardson's equation : $J = AT^2 e^{-Phi/kT}$, where J = Thermionic Current Density (A/m2); A= Thermionic Constant dependent on material properties; T = Electrode Temperature(K); Phi = Work Function of the material; k = Boltzmann Constant.

Thermionic Material. Identifying an appropriate thermionic material set for the HEAT application is very unique and difficult. Unlike typical vacuum tube applications, the package itself is subjected to a high temperature (1400 °C) thermal cycle under vacuum. This process creates a situation where the thermionic thin film material can be contaminated. This contamination will reduce the sensitivity and repeatability of this process. Since the package is enclosed, gettering this contaminated layer will be the most important factor for consistent emission current. Thus, when identifying a thermionic material for this temperature range, there are three criteria that need to be considered. First, the vapor pressure needs to be sufficiently low to prevent any residual gas interaction with the thermionic physics. Second, the material needs to be relatively inert to oxygen contamination. Third, anode and cathode cross-contamination needs to be minimized. There are few thermionic materials that have the adequate properties for this application. In addition to high temperature packaging compatibility, the work function will need to be appropriate for the temperature range.

Based on review of the relevant material properties and calculation of the resulting thermionic performance, we have selected the thermionic materials to be Lanthanum Hexaboride (LaB6), pure Tungsten (W) or Lanthanated Tungsten (W-La) . Thermionic properties of W, W-La, and LaB6 have been thoroughly studied and reported (http://erps.spacegrant.org/uploads/images/images/iepc_articledownload_1988-2007/2011index/IEPC-2011-053.pdf). Relevant properties are summarized in Table 3. LaB6 can be attained as a sheet or powder and made into a paste for patterning. The advantage of using LaB6 is that the activation process is an inherent reduction of LaB6 to metallic La. As long as the residual oxygen level is very low, LaB6 can be reduced to La with Boron gettering the residual oxygen. Otherwise, La would be oxidized to LaO. Additionally, both W and La-W can be sputtered as thin films.

Table 3. Richardson's Equation Constant and Work Function

	Lanthanated Hexaboride (LaB6)	Tungsten (W)	Lanthanated Tungsten (1% La2O3 – W)
Richardson Constant "A"	3 E5 A/m2K2	6 E5 A/m2K2	6 E5 A/m2K2
Work Function "Phi"	2.8 eV	4.5 eV	2.8 eV

Experimental Apparatus for Thermionic Data Measurement. In order to minimize the residual oxygen during data measurement, a bell jar vacuum system was modified (Figure 13). The modifications included a Niobium heater substrate for sample placement, radiant shields surrounding the heater for thermal isolation, and a small opening for electrical leads which are

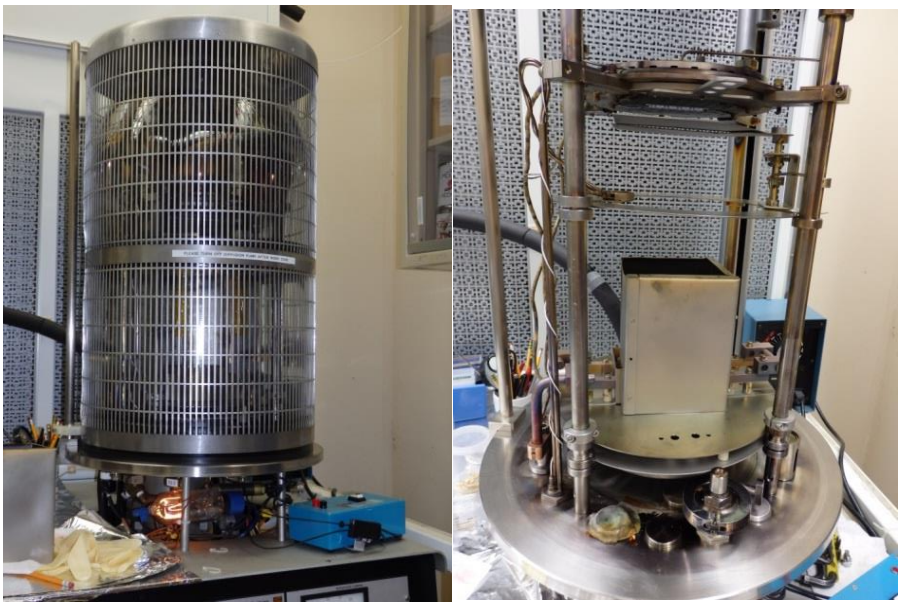

Figure 13. Modified bell jar vacuum system for thermionic measurement

used for thermionic and temperature measurements (Figure 12). Furthermore, electrical leads to measure thermionic response are sandwiched between the top and bottom electrodes while the thermocouple lead is attached to the top electrode. Overall, the system had a base pressure of 1

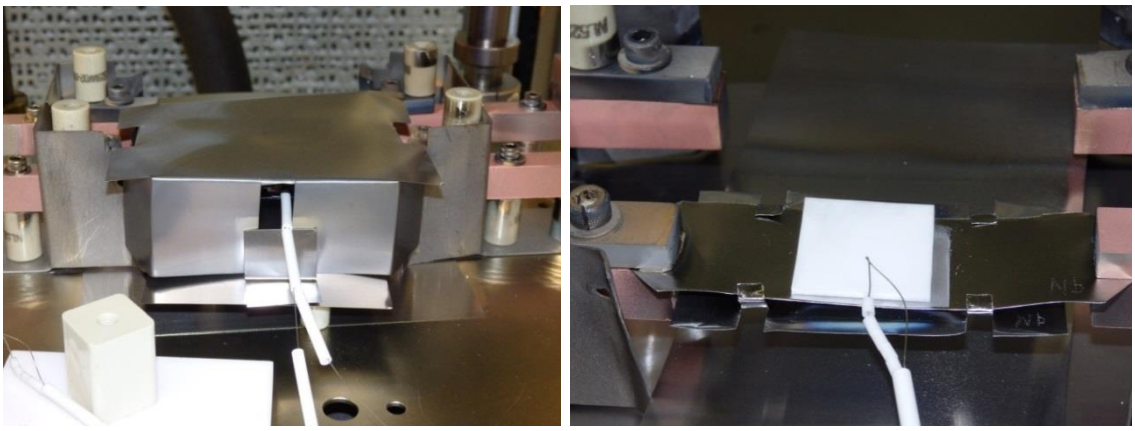

Figure 12. Radiant Heat Shield and Niobium Substrate Heater

e-7 mbar and maximum operating temperature of 1400 cel.

Thermionic Device Measurement. Thin film LaB6 substrates were fabricated using screen printed LaB6 paste on alumina substrates (Figure 14). The LaB6 patterned was a 1" diameter disk and an extended tail for a Pt wire interconnection pad. The extended tail had an additional thin film Tungsten overcoat in order to prevent Pt wire decomposition caused by Boron

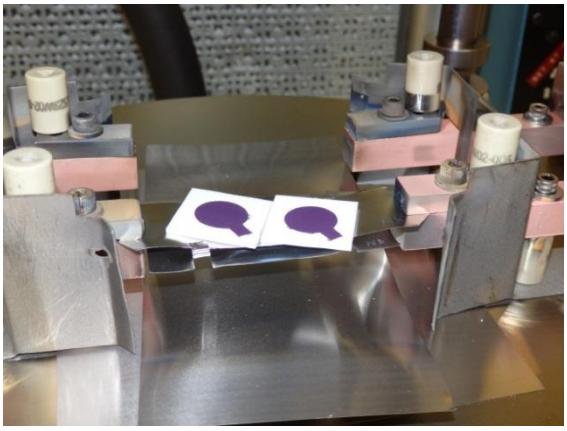

Figure 14. 1.5" Diameter LaB6 thin film

interaction. Furthermore, both the anode and cathode thermionic materials were LaB6 which minimized cross contamination. Since the device was driven using an electric field, the work function potential difference was not needed for adequate current measurement. After screen printing the LaB6 paste, the substrates were dried and baked under vacuum at temperatures up to 1300C. Further processing included a thin film Tungsten overcoat and Pt wire connection.

Thermionic data at 1200 °C for this device can be seen in Figure 15. One set represents the 1e-

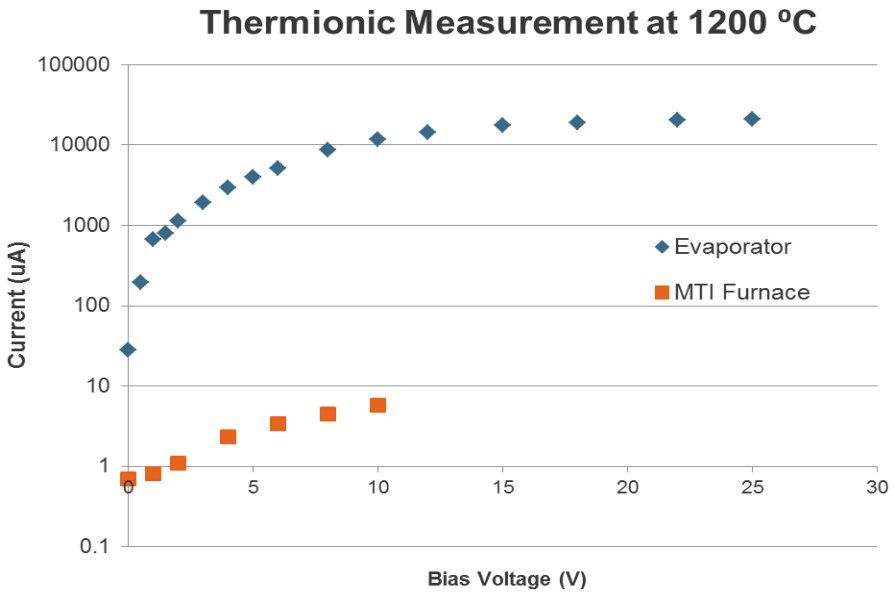

Figure 15. Thermionic Measurement using LaB6 substrates at two different base pressures. Evaporator -- 1 e-7 mbar. MTI Furnace -- 1 e-4 mbar.

7 mbar base pressure bell jar apparatus and the other a 1e-4 mbar base pressure MTI tube

vacuum furnace. A reduced base pressure environment resulted in an improved the thermionic response and repeatability.

Furthermore, device current was measured for various temperatures from 861 °C to 1125 °C (Figure 16). As the bias voltage increased, the space charge limitation was removed and the total current emission was measured. Using the Richardson/Dushman equation, the work function and Richardson constant can be calculated from the data. A work function of 2.9 eV and constant of 39 A/cm2/K2 were fitted. Both values correlate well with literature values (30 A/cm2/K2 and 2.8 eV). Since our paste was composed of polycrystalline LaB6, we expected the work function to be slightly higher than the theoretical value of 2.7 to 2.8 eV. We plan to use a work function of 2.9 eV and constant of 39 A/cm2/K2 for all further temperature calculations.

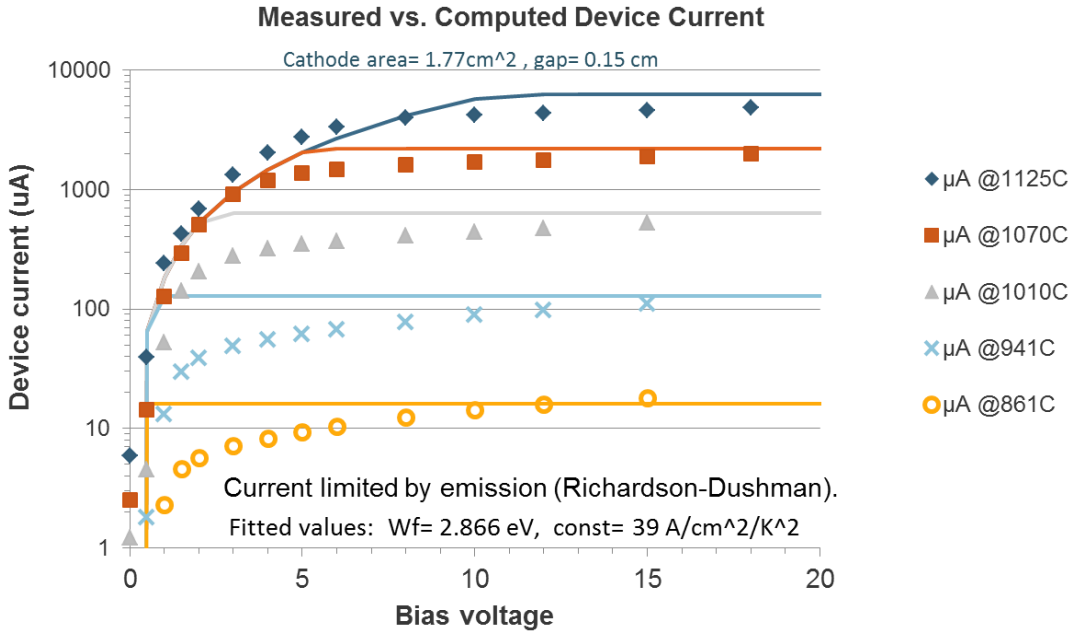

Figure 16. Thermionic Response. Experimental vs Theoretical Richardson-Dushman Current.

Data repeatability is expected to improve with a pre-conditioning high temperature step. Since the evaporator only has a maximum temperature of 1300 °C, the pre-conditioning temperature would not be optimal. Typically, devices would need to be raised above 1500 °C in order to remove all residue oxides from the surface. Any drift in data is due to this incomplete activation step.

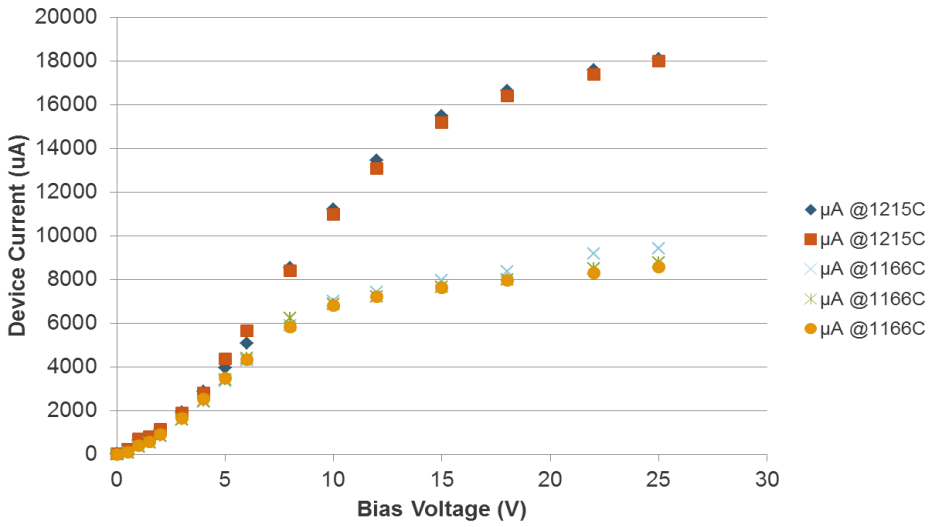

Figure 19. Repeatibilty of Thermionic Data @ 1215C and @1166C

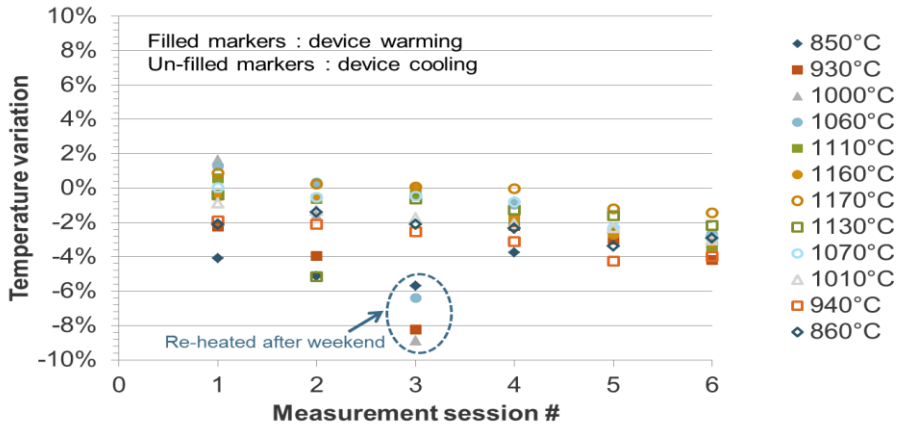

Figure 18. Day to Day Temperature Variation Measurement Sample A

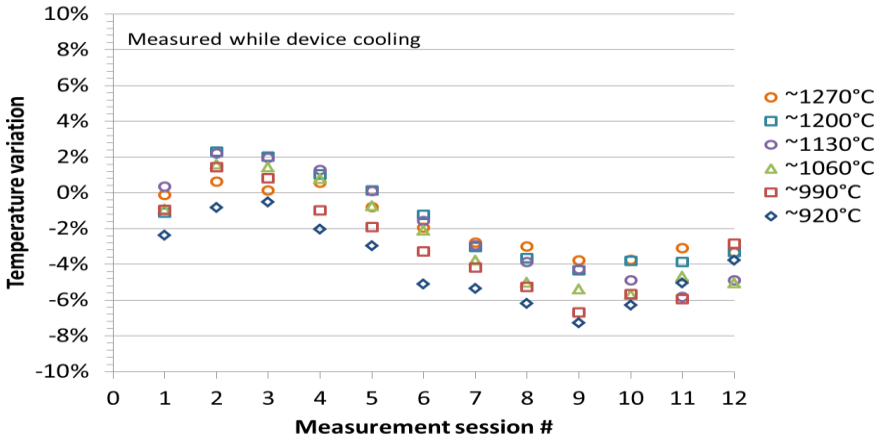

Figure 17. Day to Day Temperature Variation Measurement Sample B

Temperature variations of less than +/- 5 percent were observed for day to day runs (Figure 18

and Figure 17). Each measurement session number represents a single day run cycle starting from 850 °C to 1170 °C and back to 860 °C. All samples were heated from room temperature. To avoid thermal-shocking the alumina devices, we have been limiting the temperature changes to about 10 °C per minute, which requires small (1-2%) adjustments of power.

Hermetically Sealed Thermionic Package

Hermetically Sealed Thin Film Thermionic Compatibility. An initial survey of different thermionic material combinations for the anode and cathode were assessed. These materials included La-W, W, LaB6, ZrB2, and Barium Oxide. In summary, the two most important criteria are oxidization recovery and cross-contamination recovery. For oxidization recovery, it is a given that a thin oxide layer will form and will need to be "conditioned" at elevated temperatures. This elevated temperature can either reduce the oxide to the metal state or evaporate the oxide layer. Whether it is reduced or evaporated, this material will redeposit upon cooling to the operational temperature. Unlike the open thermionic parallel plate experiments, this system will be enclosed throughout the high temperature packaging and conditioning process. The small and confined volume will amplify the negative effect of material redeposition. This in turn will reduce the emission current and cause repeatability problems.

Getters were investigated to remove any residual oxygen and by products from the conditioning step. Zrconium (Zr) wires were placed along the edge of the thin film thermionic pattern. Ultimately only one set of material proved to be stable throughout the hermetical sealing process and film conditioning step. This material set uses LaB6 thin film paste for both the anode and cathode material. All other combinations resulted in thermionic emission of at most 10% of the expected current. As described in the previous thermionic measurement runs, an external voltage will be needed to make this sensor setup functional. In Figure 20, thermionic measurements were taken for a hermetically packaged device using LaB6 as both the anode and cathode. At the higher operating temperatures, the measured currents were consistent while at the lower temperatures redeposition of contaminates might be contributing to the current differences.

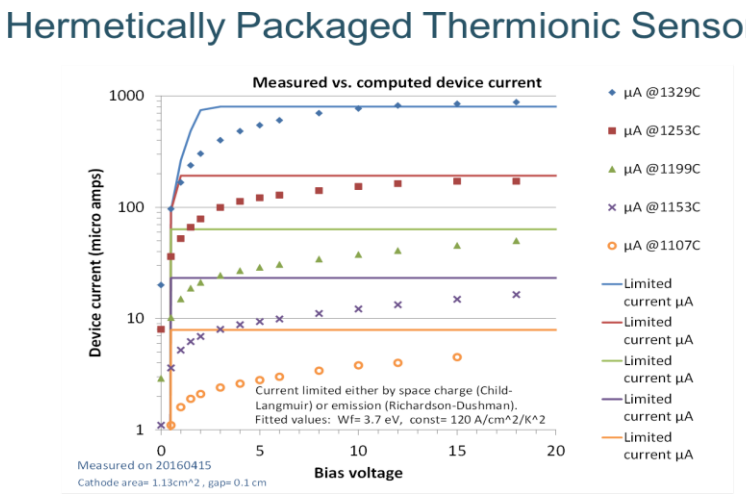

Figure 20. Thermionic Measurement of Hermetically Packaged Sensor

Designs for Pressure Thermionic Package

Pressure Membrane Dimensions and Design Rules. We have started to determine the required pressure membrane radius and thickness by calculating the total deflection of the system. A conceptual design for pressure measurements using membrane deflection can be seen in Figure 21. As either the cathode or anode layer deflects due to pressure, the gap between the electrodes will decrease. This gap change will result in a corresponding current change. Using models for a center force with clamped edge membranes, maximum deflection at the center can be calculated (Figure 22).

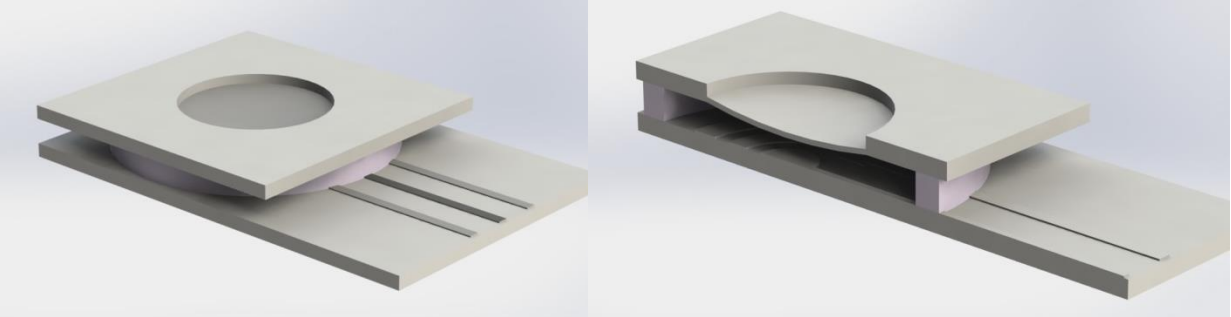

Figure 21. Conceptual Design for Thermionic Deflection Membrane

In order to have adequate sensitivity, the deflection magnitude will need to be appreciable compared to the gap distance. In Table 4. Recommended Design Thickness and Radius for Pressure Sensing

Membrane Thickness (um)	Membrane Radius (cm)	Stopper Radius (cm)	Calculated Max Deflection @ r=0 and 1 atm (um)	Calculated Max Deflection @ r=0 and 100 atm (um)
300	2.5	1.0	35	561
400	**3.0**	**1.5**	**21**	**532**
500	4.5	2.0	25	485
1000	15.0	6.0	34	545

, deflection distances for different combinations of membrane radius and thicknesses are calculated. Based upon the calculations, using a 400 um thick membrane with a radius of 3.0 cm will provide an adequate deflection range. Additionally, having the stopper radius at 1.5 cm will ensure both low and high pressures can be measured.

Table 4. Recommended Design Thickness and Radius for Pressure Sensing

Membrane Thickness (um)	Membrane Radius (cm)	Stopper Radius (cm)	Calculated Max Deflection @ r=0 and 1 atm (um)	Calculated Max Deflection @ r=0 and 100 atm (um)
300	2.5	1.0	35	561
400	**3.0**	**1.5**	**21**	**532**
500	4.5	2.0	25	485
1000	15.0	6.0	34	545

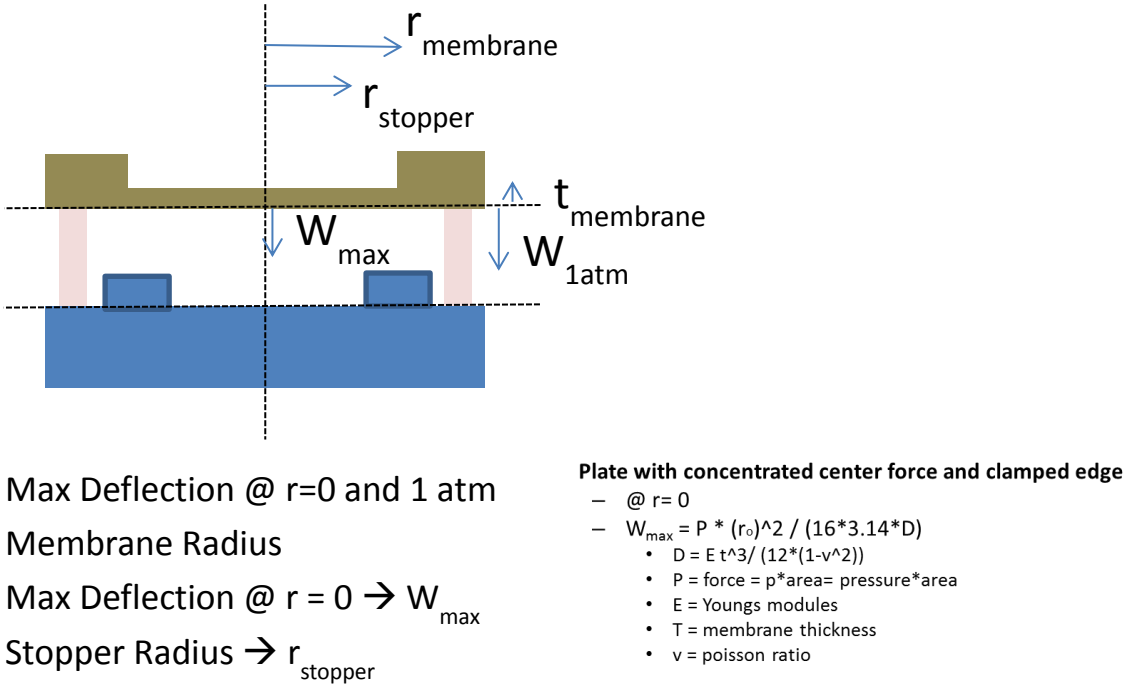

Figure 22. Model for Membrane Deflection Calculations. Eo=400 Mpa and Vo=0.27

Designs and Preliminary Tests for Self-powered Thermionic Device and Package

Intended Gasifier Design "Brick". The following schematic (Figure 23) illustrates the overall placement and design for a wireless self-powered thermionic sensor package. The wireless component of the system will be a high temperature SiC wireless circuit rated for 300 °C continuous operation. The power generation will be thermionic with the cold side on the reactor wall and hot side facing a sapphire window which will allow for radiative heating. The sensors

will be thermionic and mounted on the far end closest to the heat source. We feel that vacuum packaging the final "brick" will be similar to vacuum packaging the temperature and pressure thermionic sensors. In fact, the interconnection method will also be used to connect the SiC circuit to the thermionic devices.

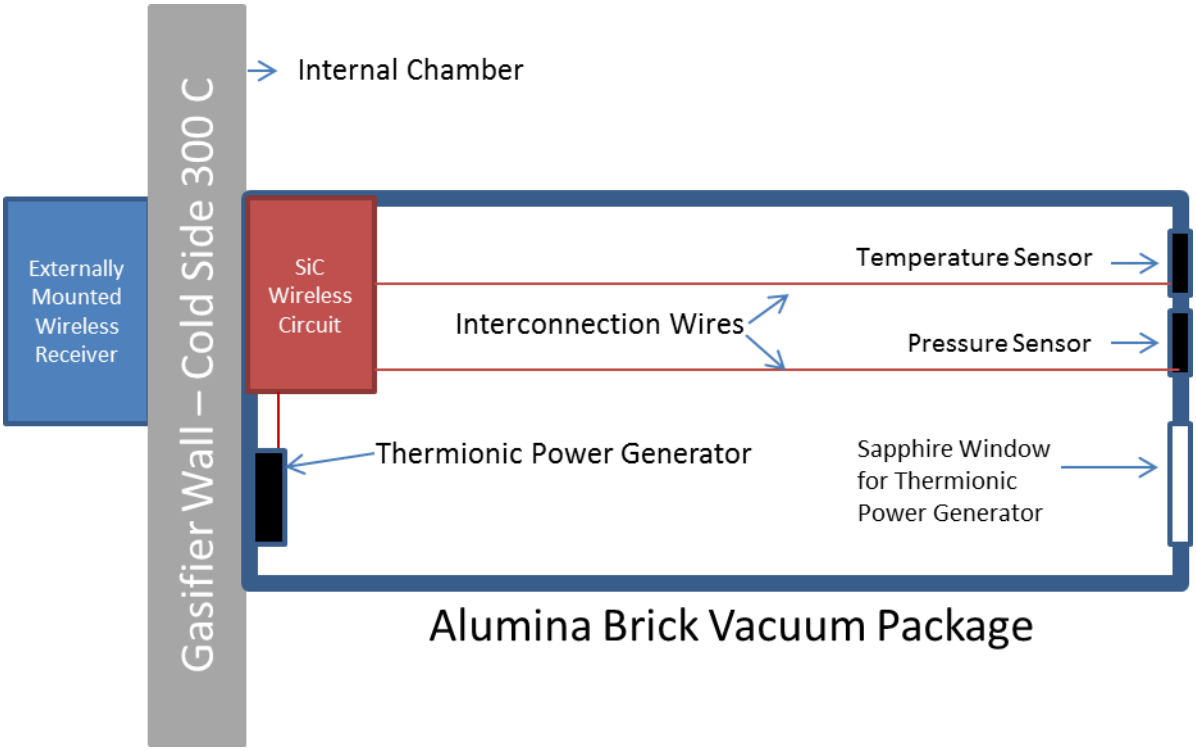

Figure 23. Schematic for a wireless self-powered thermionic sensor package.

Anode and Cathode Material Choice. The anode material will be LaB6 which has a work function of 2.9 eV in practice which is close to the theoretical work function of 2.8 eV. This data has been derived from our thermionic experiments for temperature sensing. LaB6 is replacing the original material BaO in earlier experiments. BaO has turned out to be impractical for power generation due to the high vacuum needed for operation. We plan to replace BaO with several different candidates. They are MoB2 and NdB6. We have chosen these materials (Table 5) due to published work functions that are greater than LaB6.

Table 5. Anode (coldside) Candidate Materials for Thermionic Power Generation

Material	W.F. (eV)	Comments
Refractory metals	> 4	Unsuitable for thermionic emission
ZrB_2	> 3.9	Slightly too high W.F.
MoB_2	3.7	*0.8V higher than LaB_6 measured under same conditions. (Alfa Aesar sells MoB, but not MoB_2)
NdB_6	3.2	*0.3V higher than LaB_6 measured under same conditions
ZrC	3.4 to 3.5	

* Journal of Applied Physics 54, 1076 (1983)

Anode and Cathode Temperatures. One of the key drivers for thermionic power generation is the temperature difference between the anode and cathode. We have modeled the expected thermal profile of our brick package and have concluded that the thermal difference of ~460 °C can provide adequate temperature differences for either a thermionic converter or thermoelectric device. Our lumped modeling results for temperature differences between the cathode and anode electrodes can be seen in Figure 24. The L-bar is a parameter where tungsten bars can be used to physically move the anode cathode pair closer or further away from the walls. A L-bar of zero indicates the position shown in Figure 23 and would be the optimal case. Additionally, interconnection between the anode and cathode will also provide heat losses. We have modeled the net temperature difference between the cathode and anode for various gold interconnection designs (Figure 25). The main driving force will be the interconnection area ratio between the anode and cathode. Based upon known processing capabilities, narrow interconnections can be made to maintain the thermal difference at 460 °C.

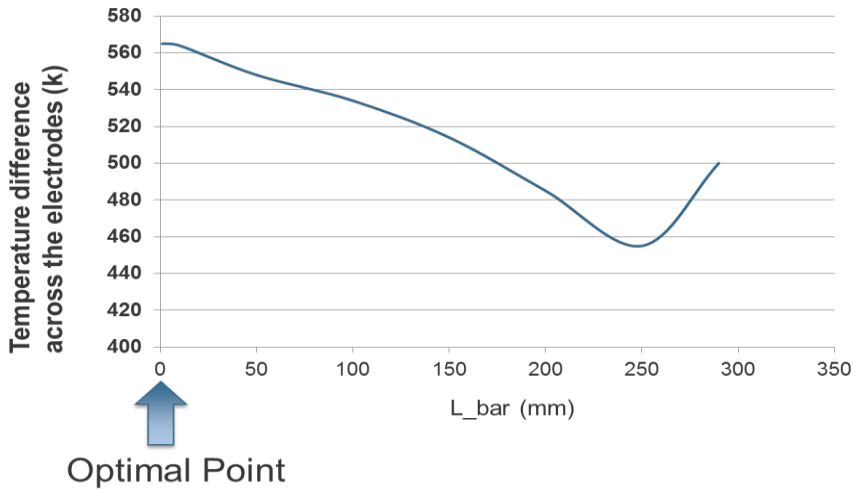

Figure 24. Thermionic Device Placement Distance from Wall

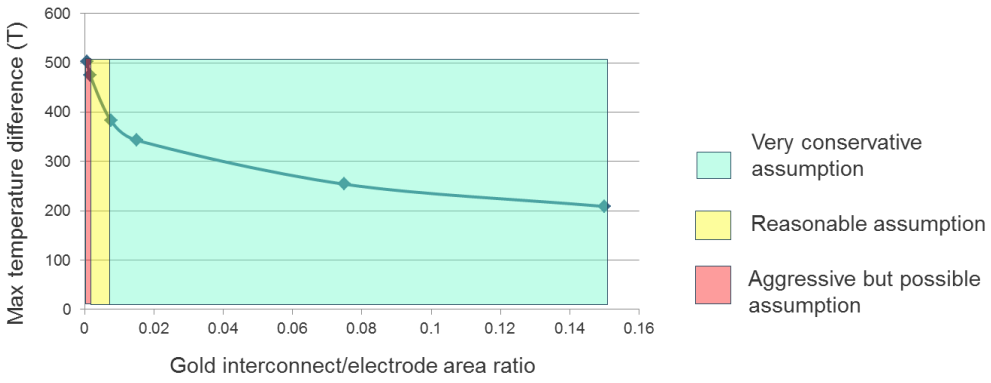

Figure 25. Gold Interconnection Area Analysis

Designs. We will validate the thermionic generator using several cathode/anode pairs. The smaller cathode/anode pairs will be assembled individually in the bell jar and placed in series to produce the desired voltage. For demonstration purposes we will pair two cathode/anode devices. The paired devices will be further packaged in a larger vacuum sealed container where the cathode will be heated using radiative heating from the tube. The overall layout and design can be seen in Figure 26 along with an initial fabricated prototype (Figure 27).

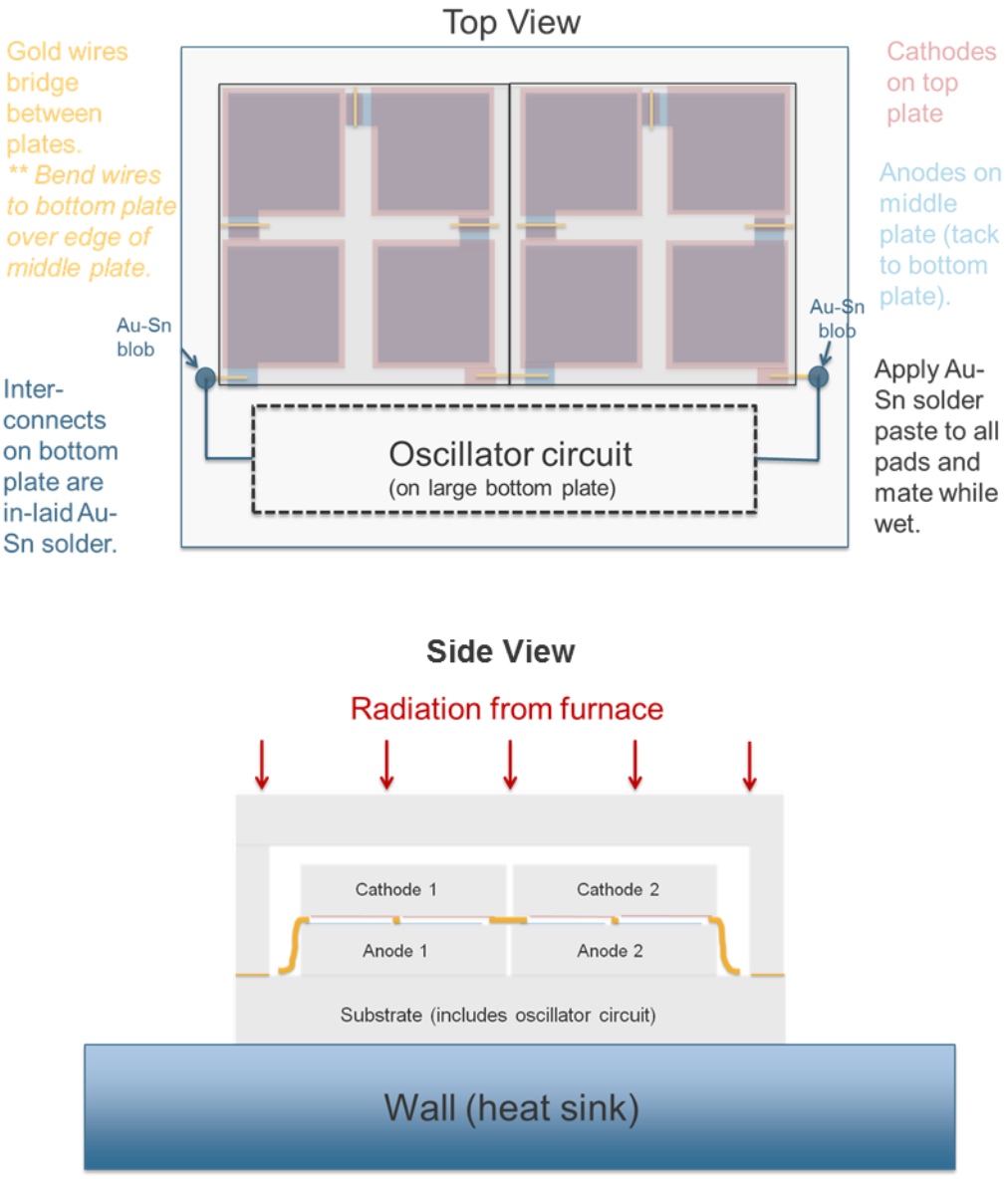

Figure 26. Layout and Design for Power Generation Device

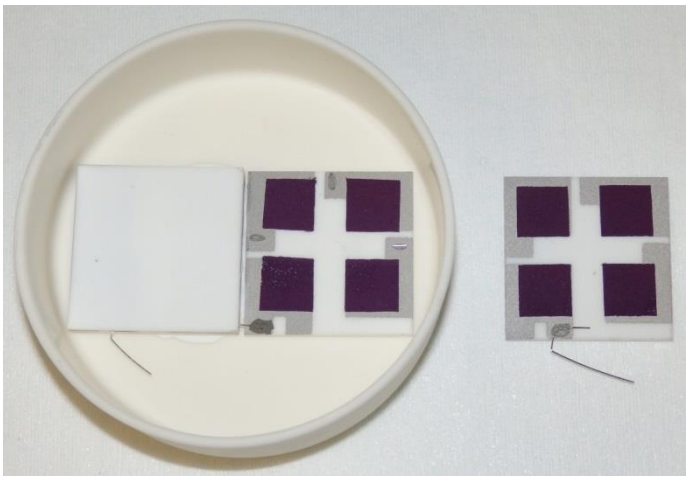

Figure 27. Fabricated Power Generation Device

Designs and Preliminary Demonstration for RF Wireless SiC Circuits

RF Wireless Simulation. In order to design the proper SiC wireless circuit, wireless simulation work was done. The simulation included a cylindrical chamber fabricated with 1 inch thick Incoloy Alloy 800 plate with fully welded seams, since this material and thickness is typically used for gasifier walls. Because normal wireless is not practical due to extremely high electrical attenuation of metal chamber to normal RF signals, we plan to utilize a magnetic coupling that is capable of overcoming the eddy currents and counter fields generated within the metal plate. This generated electro-magnetic field can be simulated and tested for wireless data transfer through the walls.

Microwave Office with Axiem method of moments solver was used to evaluate the behavior of a coupling. This simulation package is an electromagnetic solver which will allow us to predict the feasibility of our approach. The boundary condition was a completely sealed Alloy 800 box with 1 inch thick walls. Additionally, planar coaxial coils were designed for the interior and exterior walls in order to convey signals through the chamber wall (Figure 28).

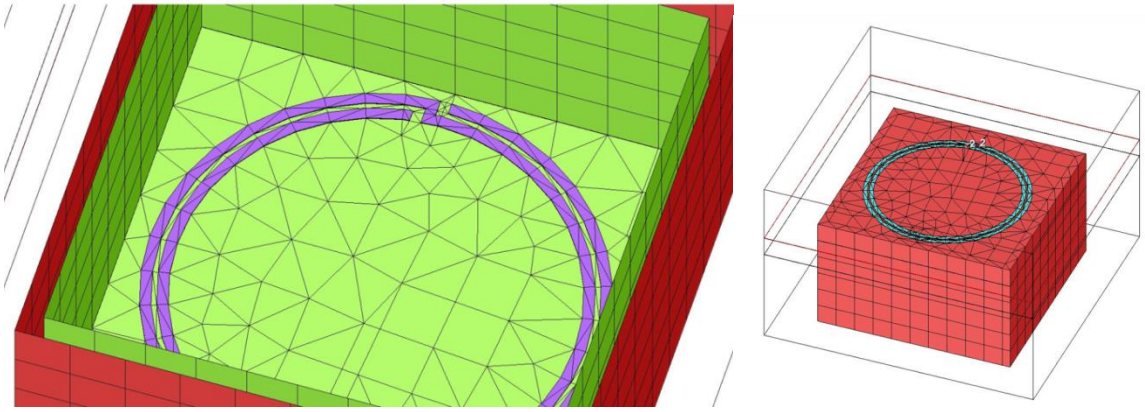

Figure 28. Axiem Simulation. Copper Planar Spiral Coil. 10 mil thick and 200 mil wide trace.

Simulation results indicate that the 8" diameter planar coils are capable of providing a link with 58 dB of attenuation at 20 kHz (Figure 29). This indicates that a 30 dBm signal would be received at -28 dBm which is a reasonable level to be detected and processed.

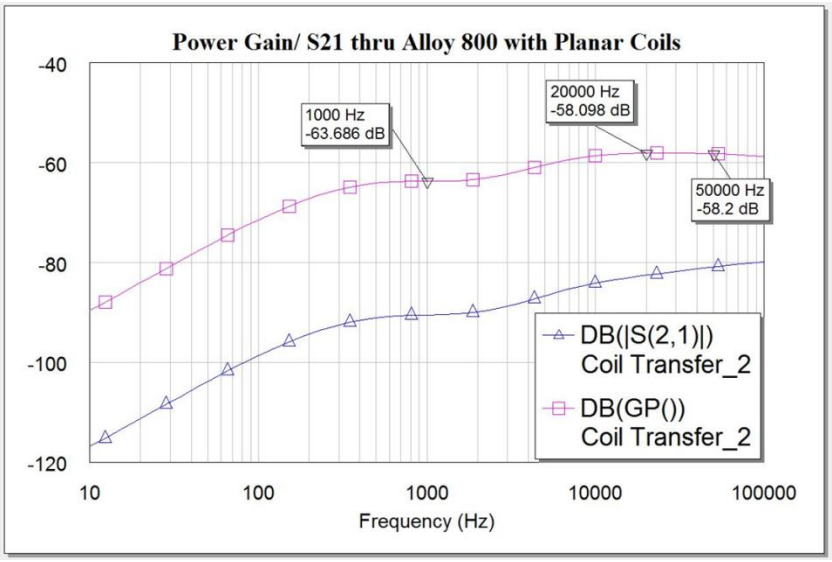

Figure 29. Axiem Results

Because the simulation showed feasibility with our design, we built and tested the SiC wireless circuit(Figure 30). For the experiment, a small signal 15 mW(12dBm) at 36 MHz was injected into the outside coil and was picked up by the matching internal coil. The signal of -94 dBm is readily detected by the spectrum analyzer (Figure 31).

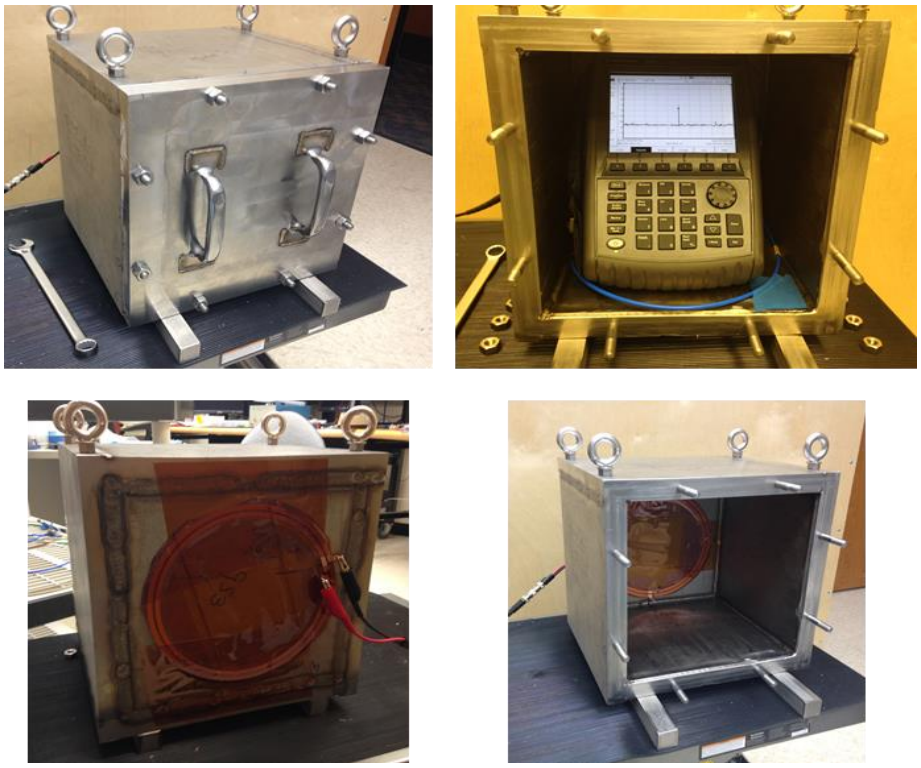

Figure 30. Experimental Test and Setup for RF Wireless Transmission.

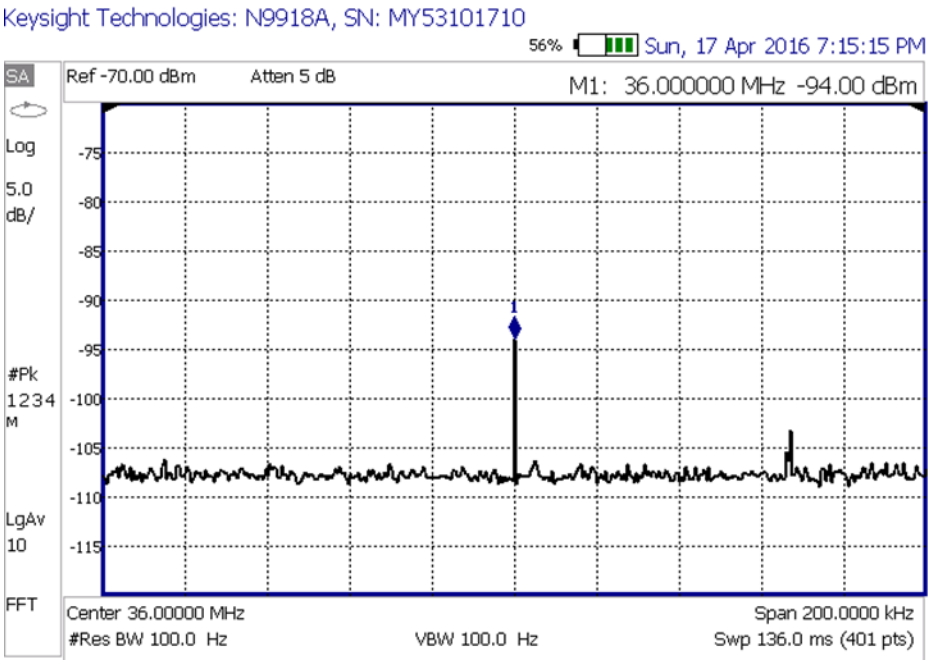

Figure 31. Measured Signal Intensity.

Thus, the overall design of the SiC wireless circuit and external receiving can be incorporated. The spiral planar coils would be mounted on a high temp substrate and bonded coaxially on the inner and outer surfaces of the chamber. A capacitive sensor would then generate a frequency deviation on a frequency modulated transmitter located inside the chamber. The transmitter would be connected to the inner planar spiral where it would generate a magnetic field that penetrates the chamber wall and is received by the outer planar spiral connected to a frequency modulated receiver. The internal circuitry would use SiC transistors, ceramic capacitors, and Ceramawire connections and air core wound inductors (Figure 32). The external circuit would use conventional electronics.

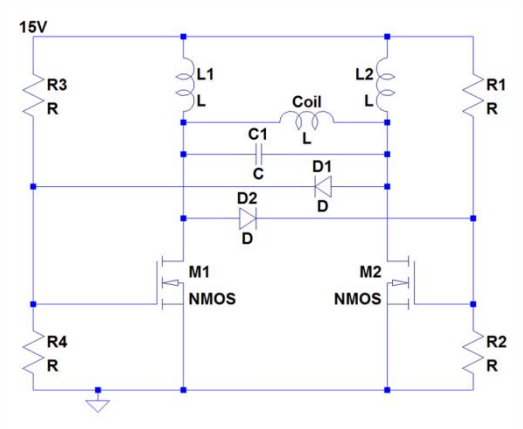

Figure 32. Simple SiC Mosfet Oscillator Design.